Supplementary Figure 1

a. Primary Screen

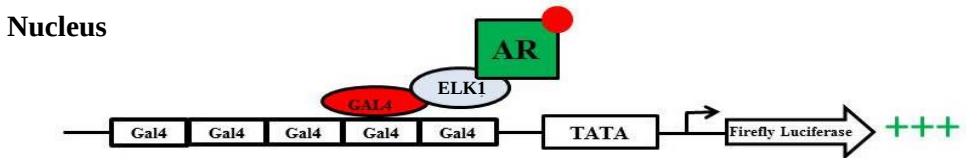

b. Counter Screen

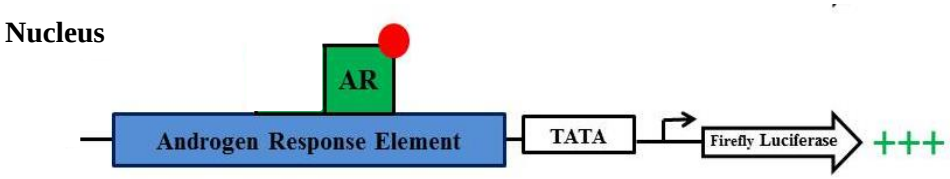

Supplementary Figure 1: (a) Schematic of the reporter system for the primary screening assay. Recombinant HeLa cells used in this assay harbor the Gal4-TATA-Luc promoter-reporter, and stably express a Gal4-ELK1 fusion protein as well as the androgen receptor (AR). Gal4-ELK1 is bound to the Gal4 elements in the promoter. In the absence of testosterone (red circle), AR is localized in the cytoplasm. When testosterone is present it binds to AR causing AR to translocate to the nucleus where it then binds to Gal4-ELK1 and activates the downstream luciferase reporter. **(b)** Schematic of the reporter system for the counter screening assay. Recombinant HeLa cells used in this assay are identical to the primary screening cells except for the absence of Gal4-ELK1 and substitution of the Gal4 elements in the promoter with a canonical ARE. In this case, testosterone causes cytosolic AR to translocate to the nucleus and bind to the ARE in the promoter resulting in activation of the luciferase reporter.

Supplementary Figure 2

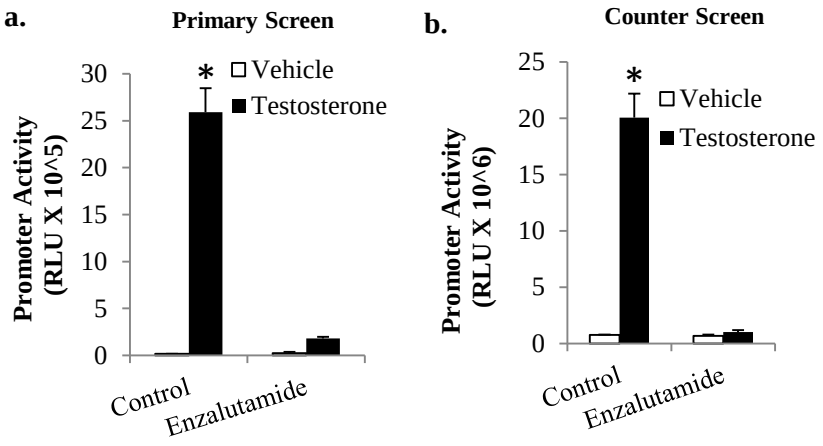

Supplementary Figure 2: Recombinant HeLa cells used in the primary screen **(a)** and in the counter screen **(b)** were treated with either vehicle (ethanol) or 10 nM testosterone together with 10uM of Enzalutamide or solvent (DMSO) control. Cells were harvested and reporter luciferase activity was measured 24 h post-treatment. In all panels, the error bars represent standard deviation of experimental triplicates. *P < 0.001

Supplementary Figure 3

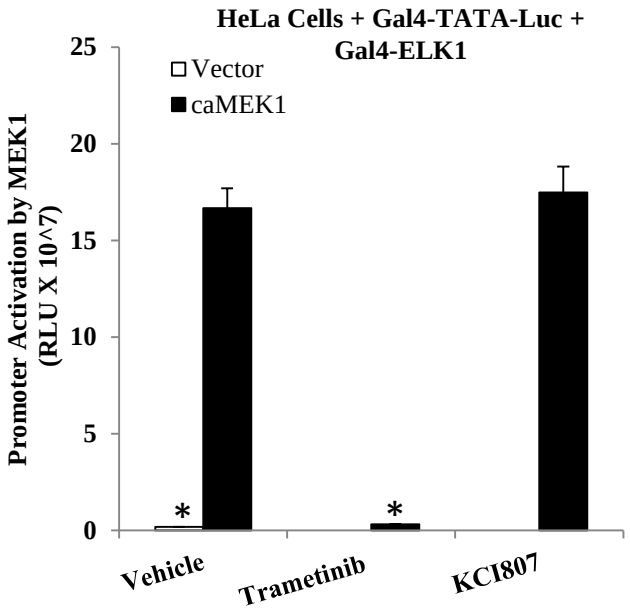

Supplementary Figure 3: HeLa cells were co-transfected with the Gal4-TATA-Luc construct and the expression plasmid for the Gal4-ELK1 fusion protein. In addition the cells were transfected with an expression plasmid for a constitutively active MEK1 protein (caMEK1). The cells were then treated with the MEK1 inhibitor, trametinib (1 μM), KCI807 (20 μM), or vehicle (DMSO). Cells were harvested 48h post transfection and luciferase activity was measured. In all panels, the error bars represent standard deviation of experimental triplicates. *P < 0.001

Supplementary Figure 4

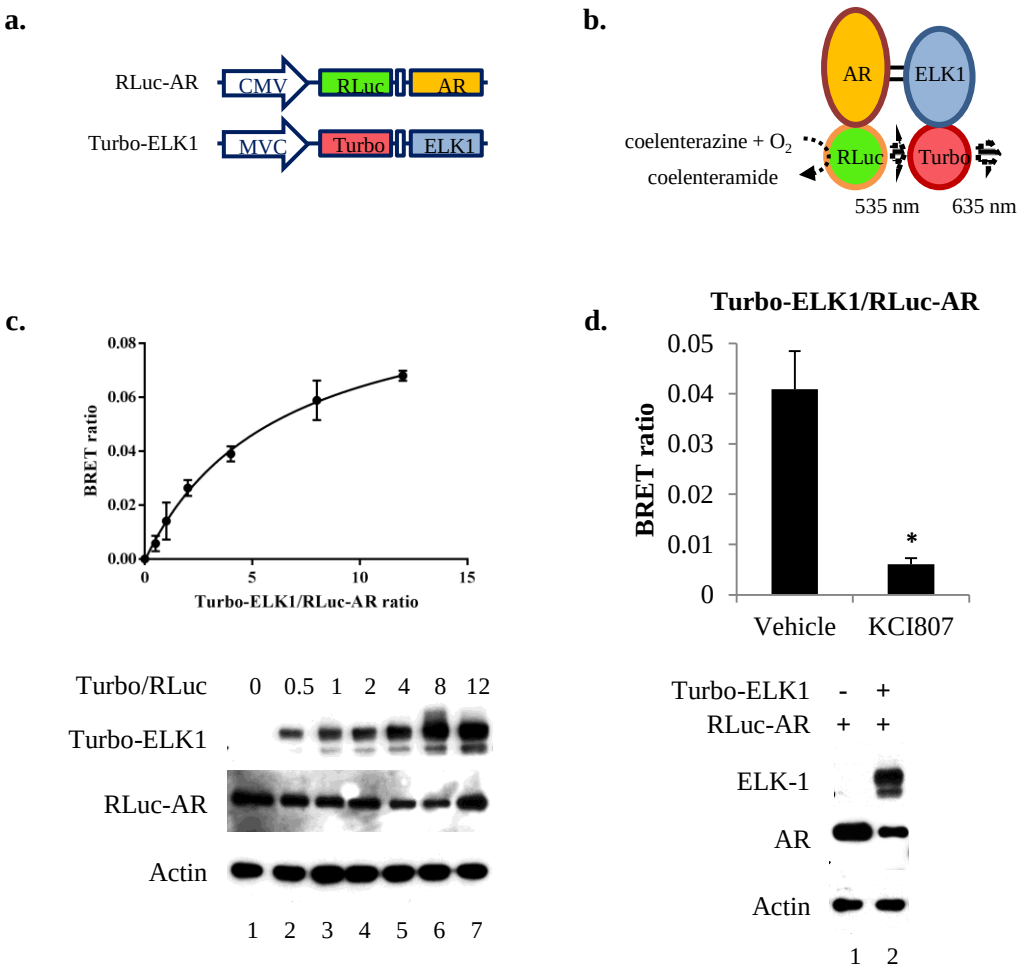

Supplementary Figure 4: (**a**) Diagram of constructs used in BRET assays. RLuc, RLuc8.6 luciferase; Turbo, Turbo635 fluorescent protein. (**b**) Schematic showing principle of BRET assay. (**c, top**) BRET assay confirmation of AR-ELK1 interactions in HEK293T cells transfected with AR and ELK1 fusions at different ratios. BRET signals were measured 1 h after coelenterazine addition. **(c, bottom)** Representative AR and ELK1 protein expression (**d, top**) Effect of KCI807 (10μM) compared to Vehicle (DMSO) on AR-ELK1 interactions in HEK293T cells transfected with Turbo-ELK/Rluc-AR at 5:1 ratio. (**d, bottom**) Representative AR and ELK1 protein expression. *P< 0.001

Supplementary Figure 5

a.

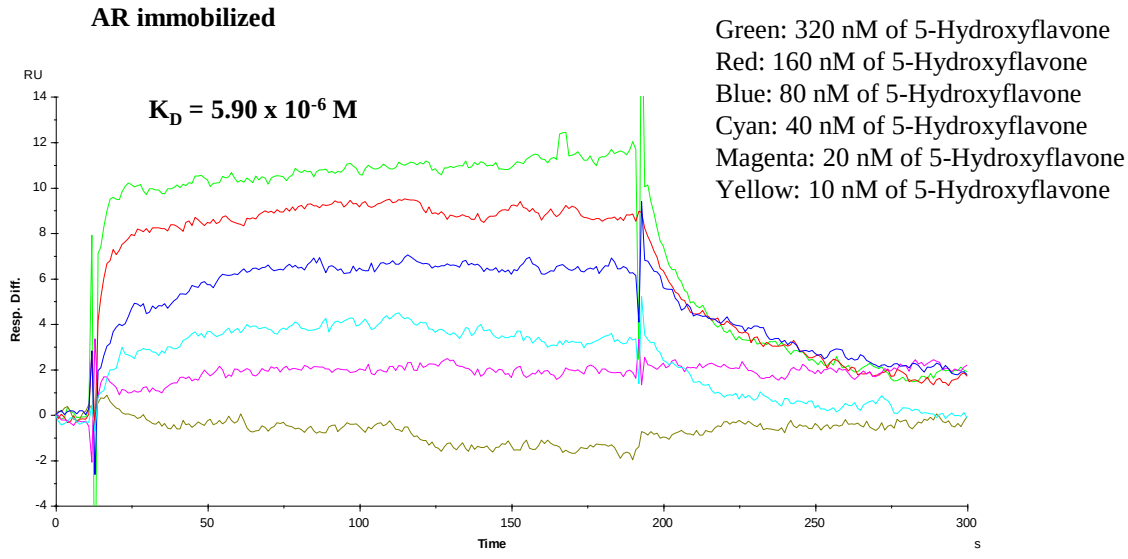

b.

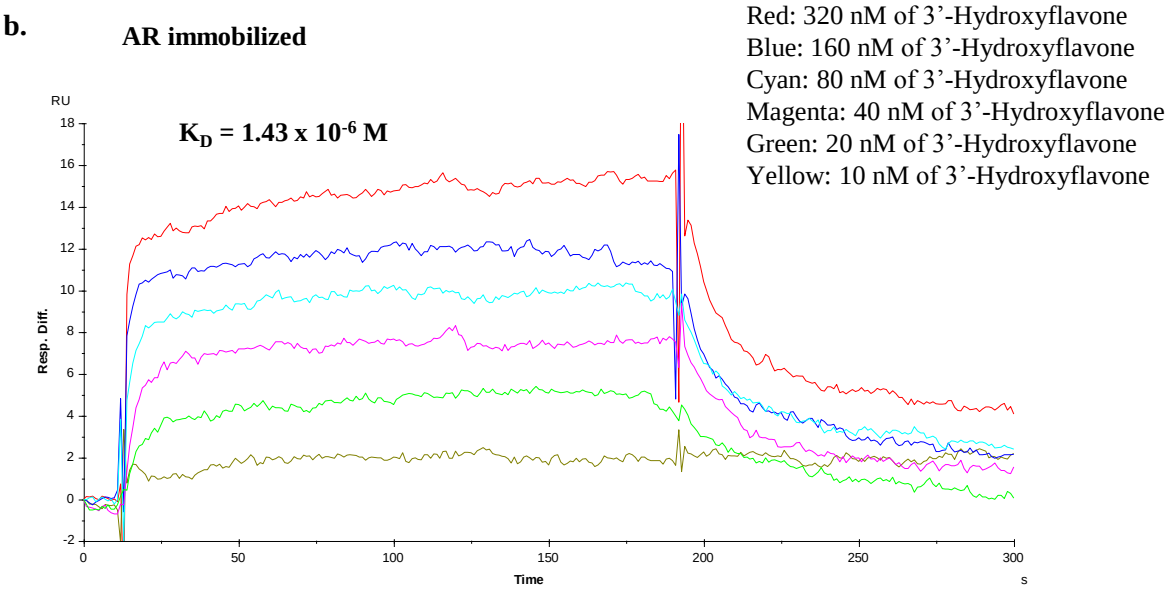

Supplementary Figure 5: Surface plasmon resonance (SPR) kinetic curves for quantitative analyses of compounds binding to AR. AR was immobilized and the compound (analyte) was diluted in a series (0, 10, 20, 40, 80, 1600, and 320nM). (**a**) 5-Hydroxyflavone was used as the analyte (**b**) 3'-Hydroxyflavone was used as the analyte.

Supplementary Figure 6

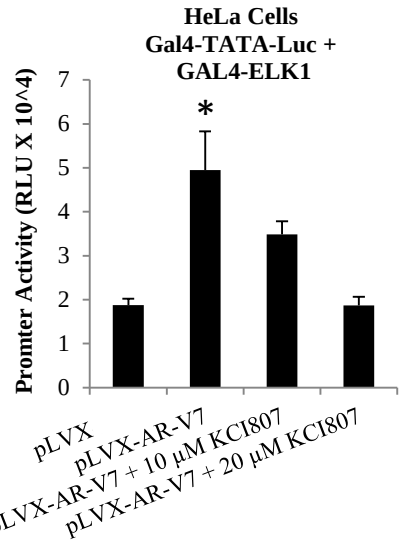

Supplementary Figure 6: HeLa cells were co-transfected with the Gal4-TATA-Luc construct and the Gal4-ELK1 fusion protein expression plasmid. The cells were also co-transfected with either the AR-V7 expression plasmid (pLVX-AR-V7) or the corresponding vector plasmid (pLVX). At the time of transfection with AR-V7, the cells were also treated with KCI807 (10 uM or 20 uM) or with the vehicle control. Promoter activity was measured in terms of reporter luciferase activity. In all panels, the error bars represent standard deviation of experimental triplicates. *$P < 0.05$

Supplementary Figure 7

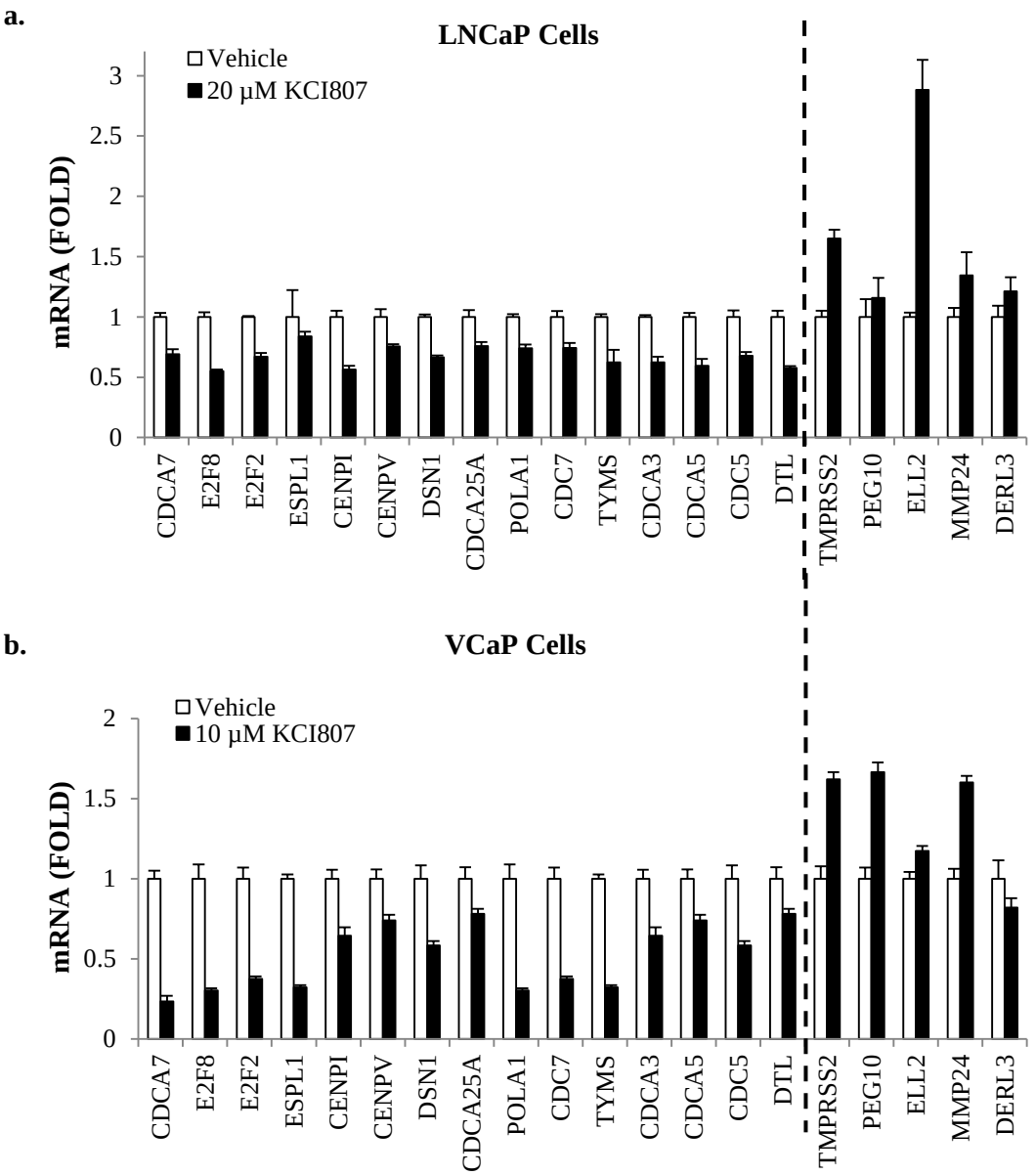

Supplementary Figure 7: (a) LNCaP cells or **(b)** VCaP cells were treated with 20 or 10 µM of KCI807 for 72h and real time RT-PCR was used to measure mRNAs for the indicated panel of genes tested. Genes on the left of the dashed line in panels **a** and **b** are those that require ELK1 for activation by AR and those on the right of the dashed line are ELK1-independent AR target genes.

Supplementary Figure 8a-b

a.

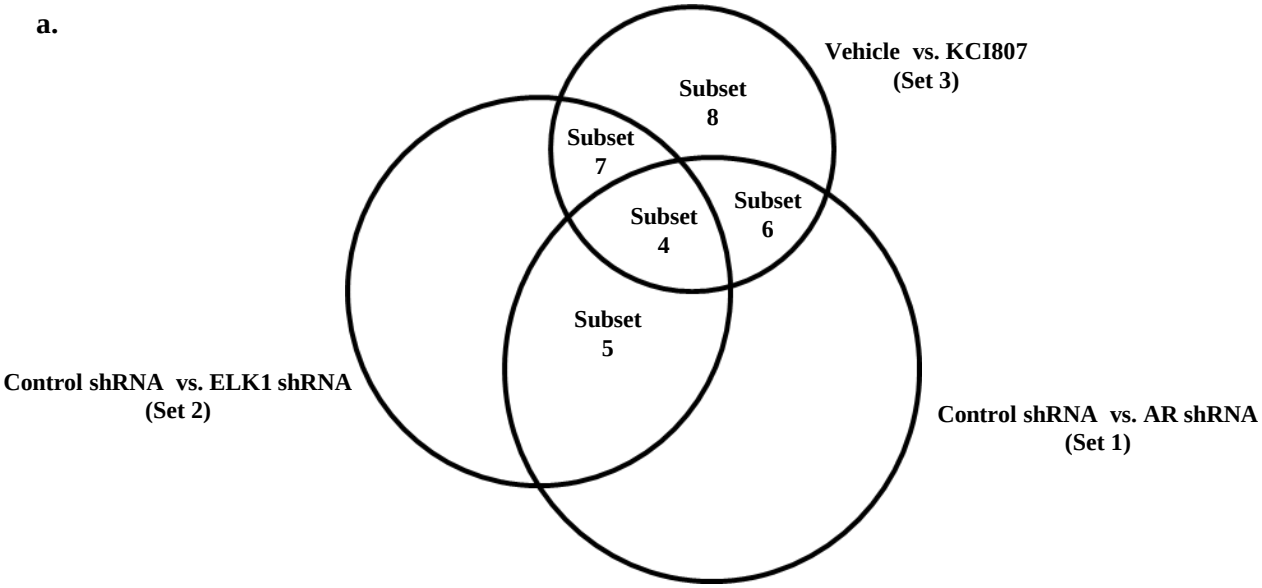

b.

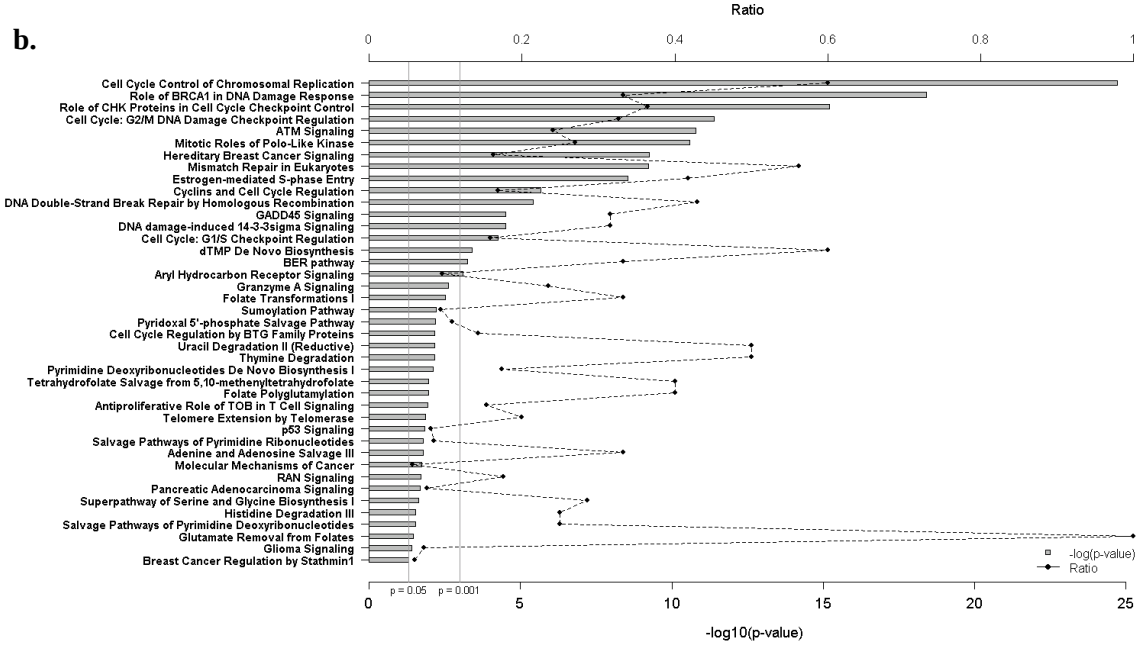

Supplementary Figure 8c-d

c.

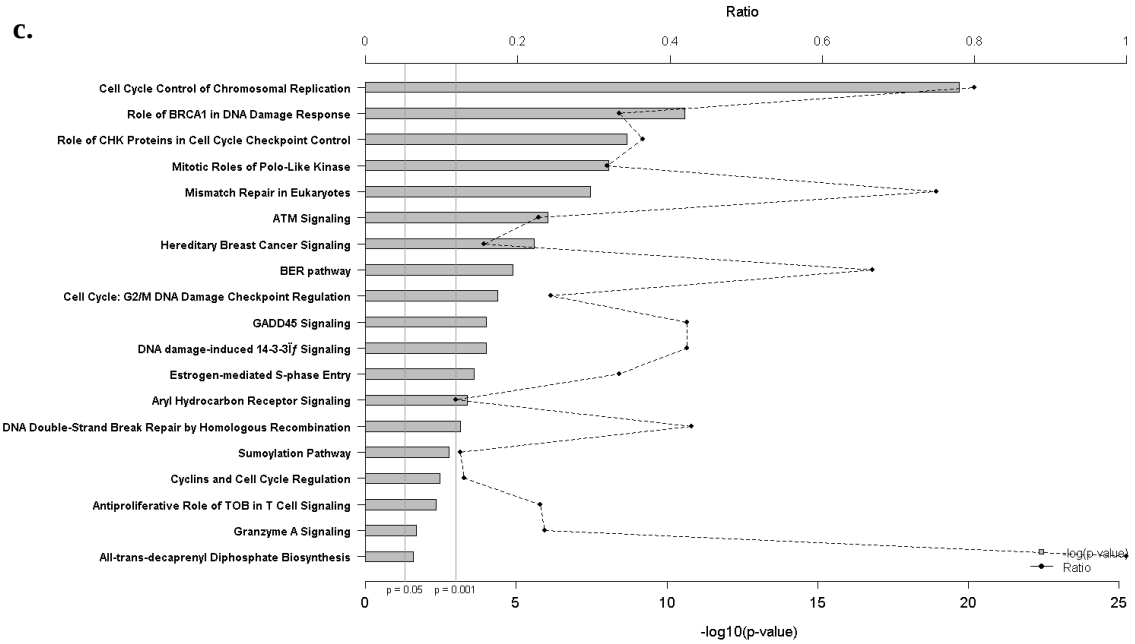

d.

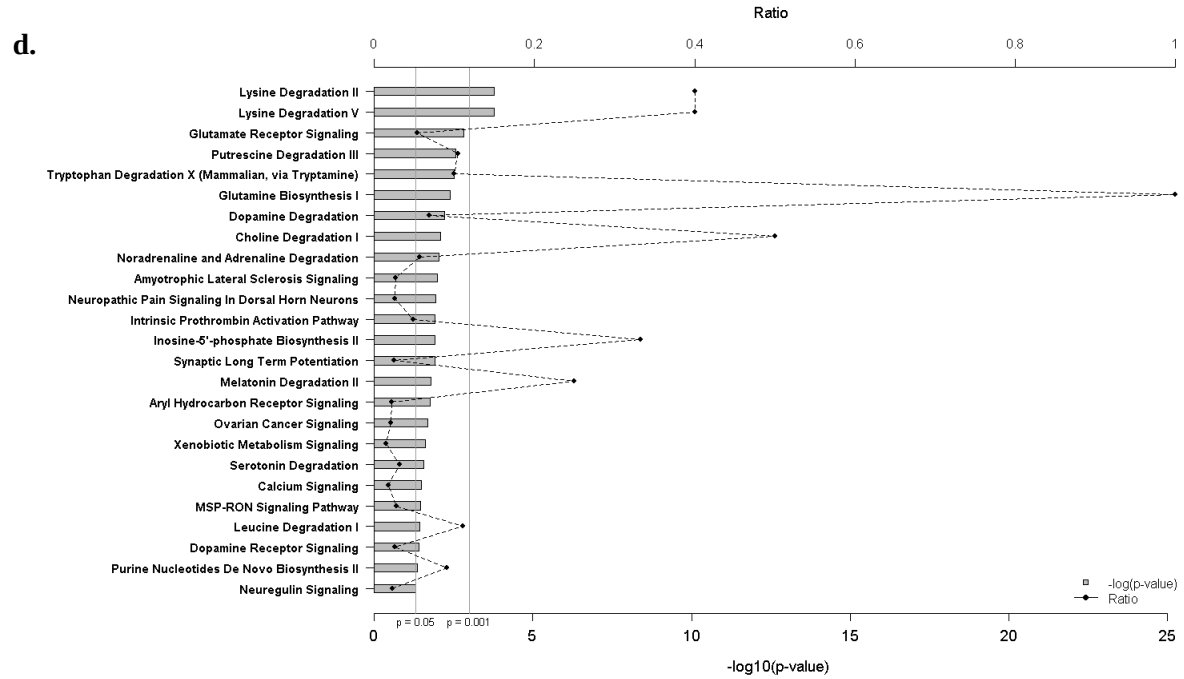

Supplementary Figure 8e

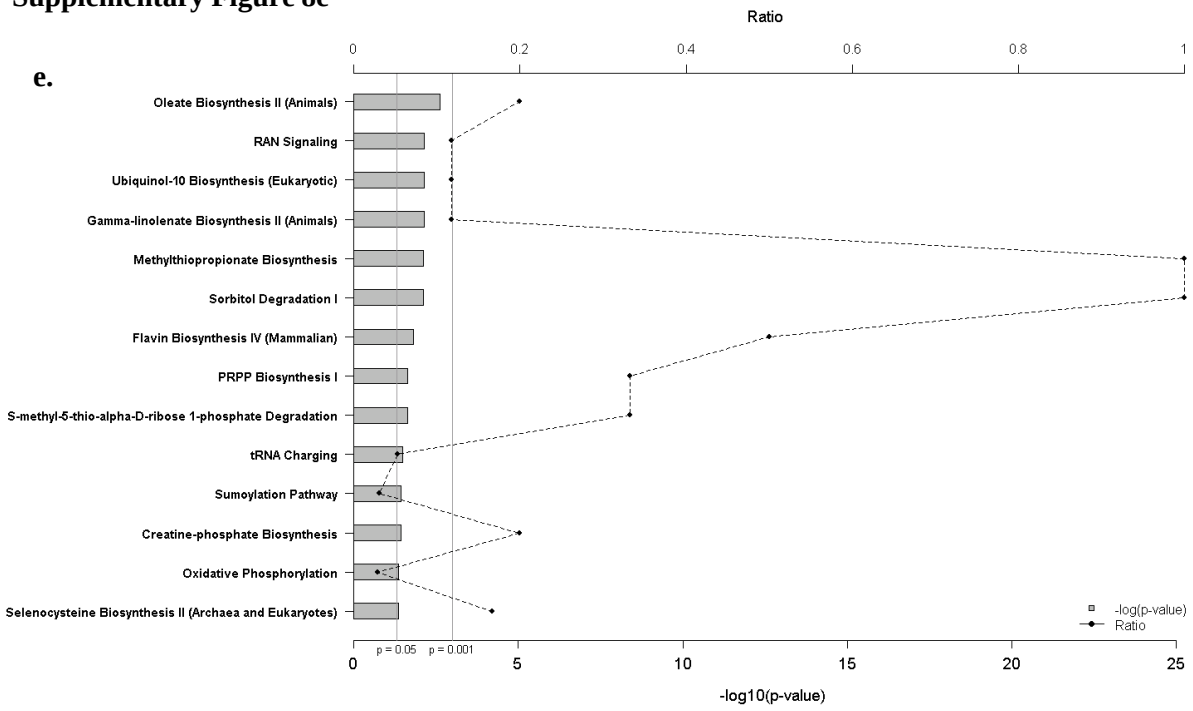

Supplementary Figure 8: Canonical pathways of differentially expressed gene sets in 22Rv1 cells. (a) Venn diagram representing sets of genes whose expression is elevated (≥ 2-fold) in control shRNA vs. ARshRNA (Set 1), control shRNA vs. ELK1shRNA (Set 2) and vehicle vs KCI807 (Set 3). (b) All ELK1-dependent AR target genes (intersecting subsets 4 + 5 in Panel a). (c) ELK1-dependent AR target genes suppressed by KCI807 (intersecting subset 4 in Panel a). (d) ELK1-independent AR target genes suppressed by KCI807 (intersecting subset 6 in Panel a). (e) Off-target genes (genes not activated by AR) suppressed by KCI807 (subsets 7 + 8 in Panel a). In Panels b-e, the gene subsets were analyzed by IPA for canonical pathways and statistically significant canonical pathways are depicted (p-value < 0.05). Bars (lower x-axis) indicate –log10(p-value) and solid circles (upper x-axis) indicate the ratio of molecules present in the dataset vs all molecules with related functions. Two vertical grey lines indicate p-values of 0.05 and 0.001. The p-value reflects the likelihood that the association between significantly differentially expressed molecules from experiments and those from a database is due to random chance..

Supplementary Figure 9

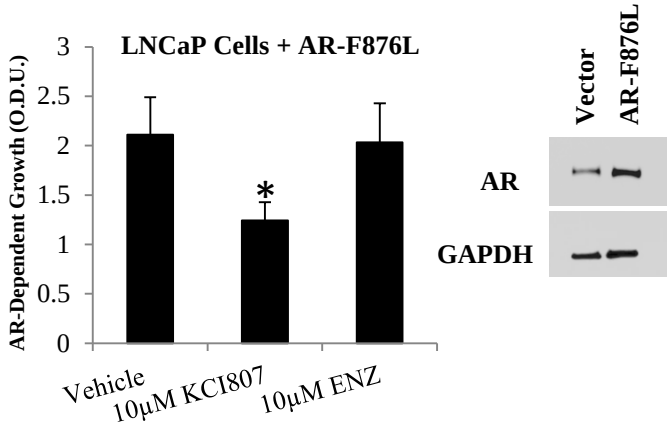

Supplementary Figure 9: LNCaP cells were transduced using lentivirus expressing the AR F876L. After 72 h, cells were plated in 96-well plates, in the presence of vehicle, KCI807 (10 uM) or enzalutamide (ENZ, 10 uM). Cell growth was measured by the MTT assay at the end of 5 days. The inset shows western blot analysis of cell lysates, 72 h post-infection, probed with antibody to AR or with antibody to GAPDH (loading control).

Supplementary Figure 10

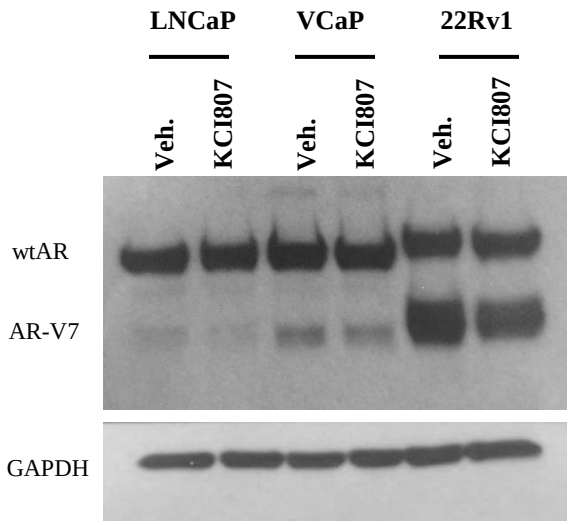

Supplementary Figure 10 : LNCaP, VCaP, and 22Rv1 cells were treated with vehicle or KCI807 (10 μM). Protein lysates were extracted after 24h of treatment and probed using antibodies to AR and GAPDH (loading control).

Supplementary Figure 11

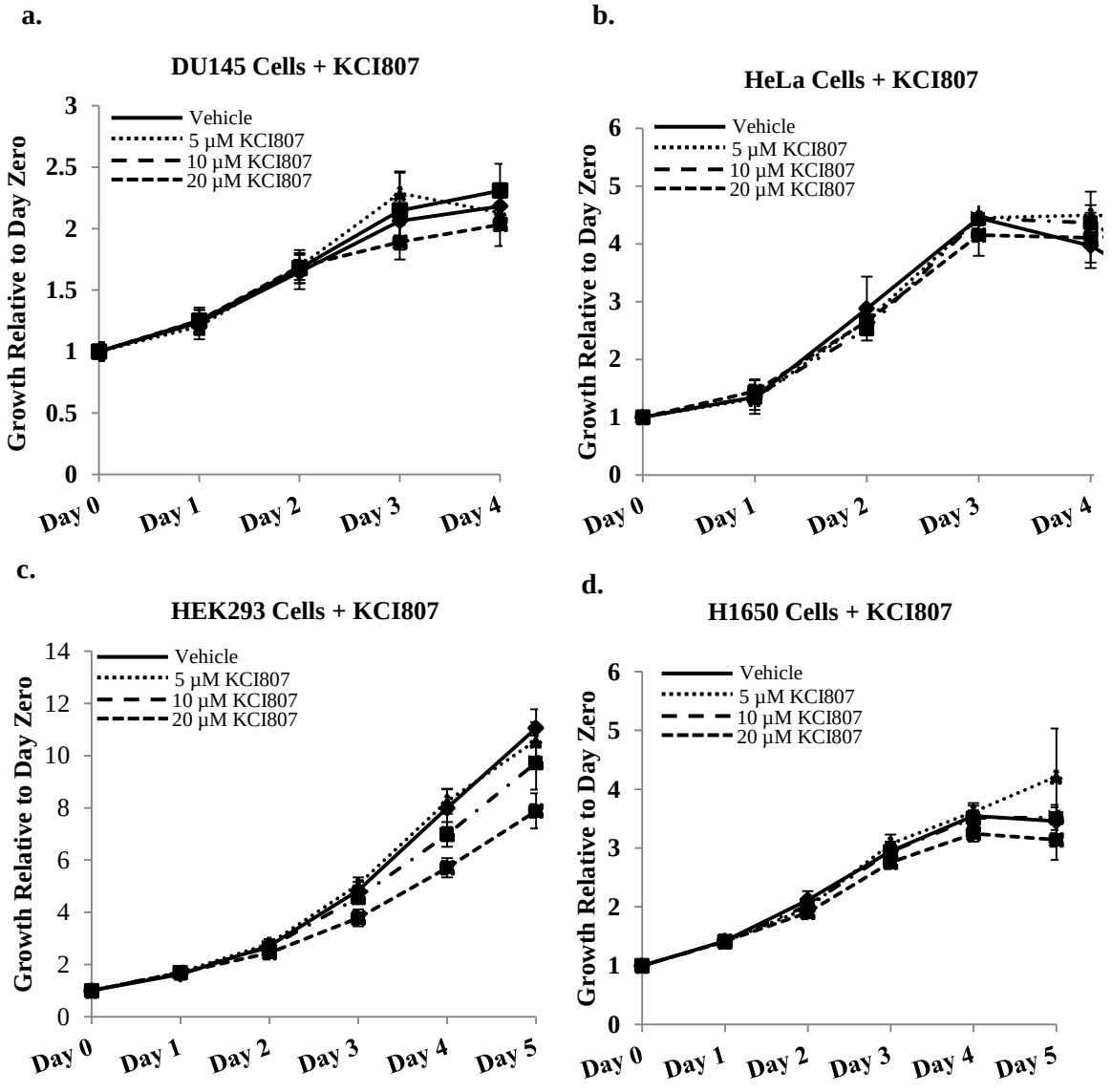

Supplementary Figure 11: Effect of KCI807 on *in vitro* growth of AR-negative cell lines was measured by the MTT assay. All values were plotted relative to the Day zero value for each cell line: **(a)** Du145 cells **(b)** HeLa cells **(c)** HEK293 cells **and (d)** H1650 cells.

Supplementary Figure 12

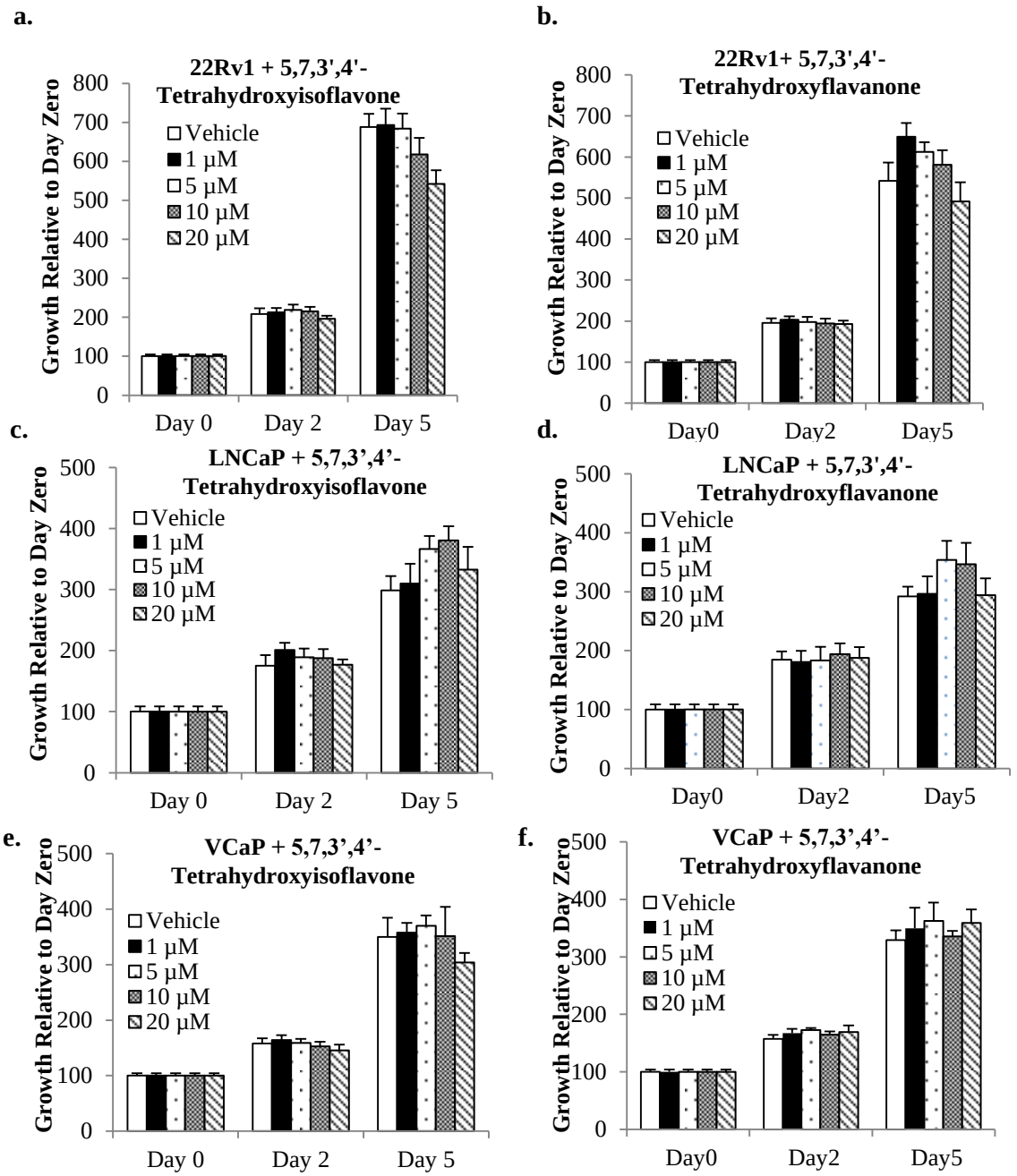

Supplementary Figure 12 : The effect of 5,7,3',4'-tetrahydroxyisoflavone and of 5,7,3',4'-tetrahydroxyflavanone on the growth of various prostate cancer cell lines was tested using the MTT assay. Twenty four hours after plating the cells, they were treated with the indicated concentrations of each compound. The data are shown in the following order: 22Rv1 Cells + 5,7,3',4'-tetrahydroxyisoflavone **(a)** 22Rv1 Cells + 5,7,3',4'-tetrahydroxyflavanone **(b)** LNCaP Cells + 5,7,3',4'-tetrahydroxyisoflavone **(c)** LNCaP Cells + 5,7,3',4'-tetrahydroxyflavanone **(d)** VCaP cells + 5,7,3',4'-tetrahydroxyisoflavone **(e)** VCaP cells + 5,7,3',4'-tetrahydroxyflavanone **(f).** In no case did either compound show a statistically significant effect on cell growth.

Supplementary Figure 13

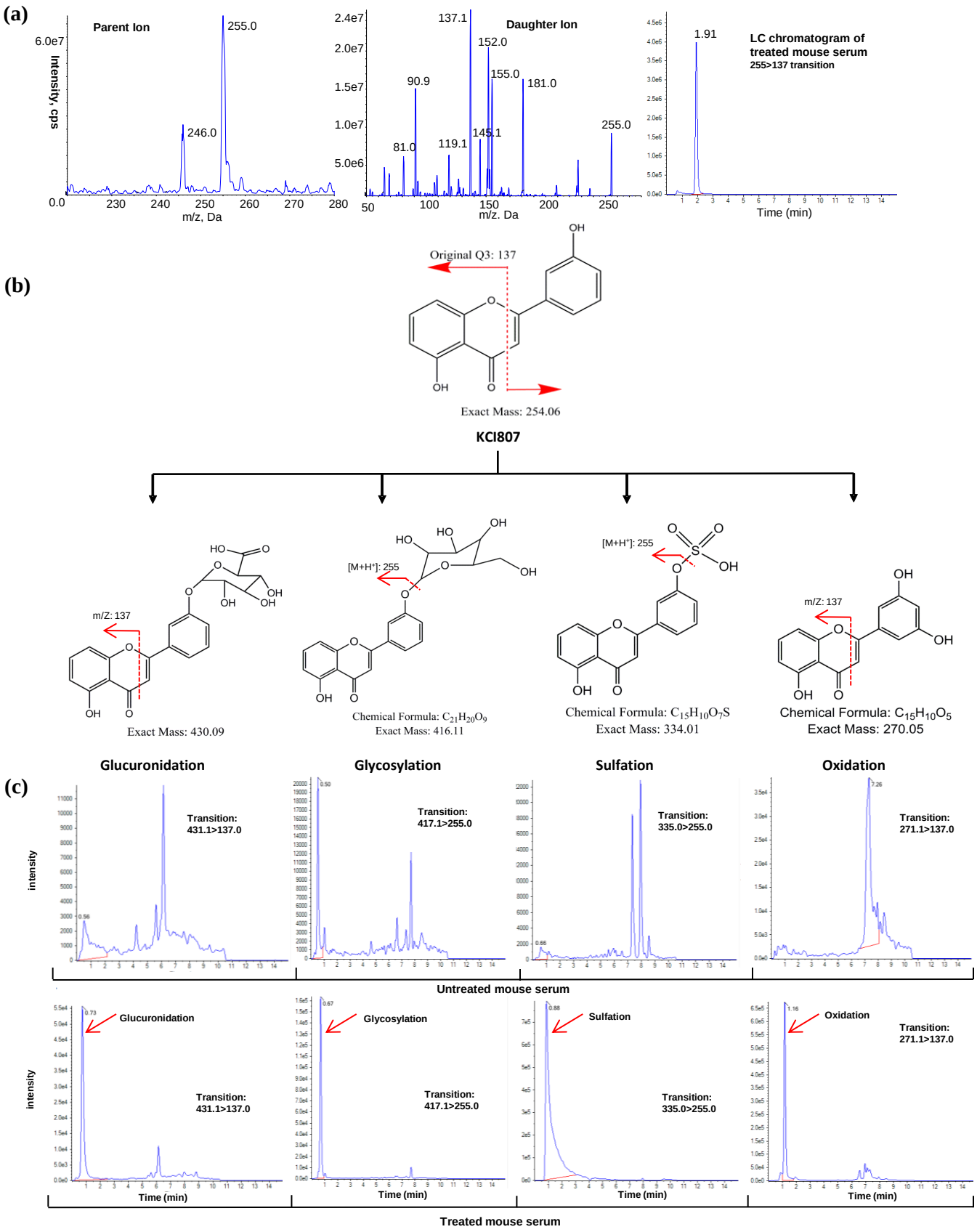

Supplementary Figure 13: Proposed metabolic pathway of KCI807. (A) Mass spectra of KCI807 parent ion and product ions, and the chromatogram of KCI807 reference standard (50 nM) monitored at the most sensitive mass transition (m/z, 255.0 > 137.0). (B) Chemical structures and major fragmented position for KCI807 and potential metabolites detected in the KCI807-treated mouse serum samples. (C) Chromatograms of the drug-treated and untreated mouse plasma samples, monitored at the theoretical mass transitions for potential metabolites.

Supplementary Figure 14

a.

Monitoring body weights of male SCID mice harboring 22Rv1 tumor xenografts in Figure 5a

Days After Tumor Implantation	0	6	11	14	17	20	24	25
Diluent Control % body weight lost/gained	0	+2.8	+4.6	+1.9	+3.7	+4.6	+3.7	+3.7
Enzalutamide % body weight lost/gained	0	+3.7	+5.5	+3.7	+4.6	+4.6	+4.6	+3.7
KCI807 % body weight lost/gained	0	-1.87	+.09	0	0	+2.7	+3.5	+2.7

b.

Monitoring body weights of male SCID mice harboring PDX-PR011 tumor xenografts in Figure 5b

Days After Tumor Implantation	1	2	3	4	5	6	7	8	9	10	11	12
Diluent Control % body weight lost/gained	0	-1.5	-3.8	-1.5	-0.8	0	+0.8	+0.8	+3.1	+2.3	+3.8	+5.3
KCI807 % body weight lost/gained	0	-3.8	-4.6	-2.3	-2.3	-1.5	0	-1.5	+0.8	+0.8	+1.5	+3.1

c.

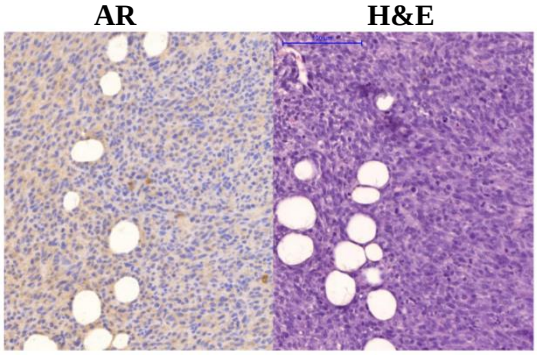

Supplementary Figure 14: In a and b, monitored body weights of mice used in the experiments described in Figures 5a and 5b, respectively are tabulated. In c, the PDX-PR011 tumor from serial passage 8 obtained from the mouse host was sectioned and stained by immunohistochemistry (IHC) to detect AR (Left panel); the right panel in c shows staining with hematoxylin and eosin. IHC performed by the KCI Bio-Specimen Core.

Supplementary Figure 15

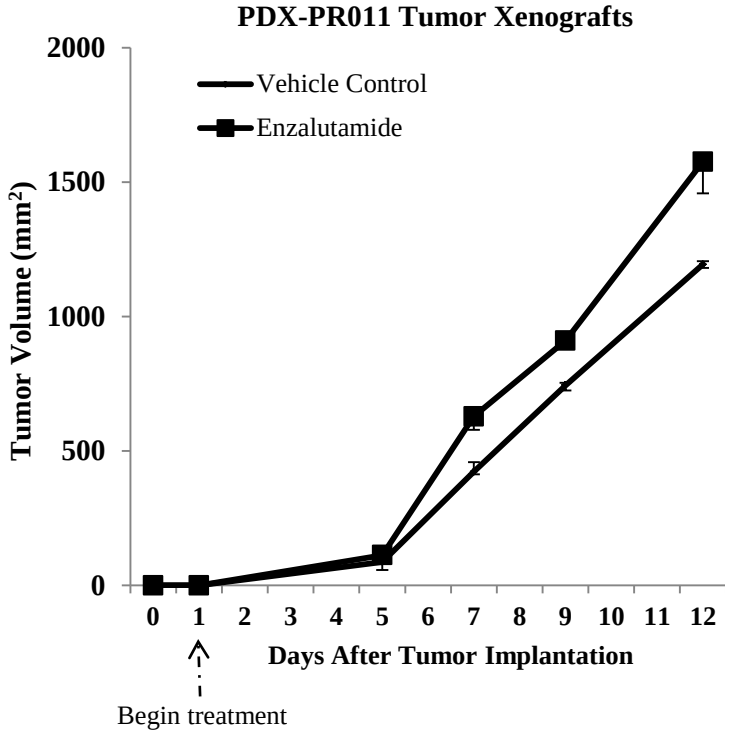

Supplementary Figure 15: PDX-PR011 tumor xenografts were implanted sc into male SCID mice in both flanks. Enzalutamide was administered following the standard regimen of daily oral administration of 50mg/Kg. Treatment was begun on Day 1 after tumor implantation. Tumor volume curves are plotted as median and an interval of semi-interquartile range on the basis of their raw values.